



## Supplementary Materials for

### **Mammalian oocytes store mRNAs in a mitochondria-associated membraneless compartment**

Shiya Cheng *et al.*

Corresponding author: Melina Schuh, melina.schuh@mpinat.mpg.de

*Science* **378**, eabq4835 (2022)

DOI: 10.1126/science.abq4835

#### **The PDF file includes:**

Figs. S1 to S15

#### **Other Supplementary Material for this manuscript includes the following:**

Movies S1 to S10

Data S1 to S6

MDAR Reproducibility Checklist

**A** Highly expressed RNA-binding proteins in mouse oocytes

Rank_1000oo_rep1	Rank_1000oo_rep2	Protein names	MARDO localization
23	23	YBX2	Yes
93	87	DDX19A, DDX19B	Not analyzed
94	86	PABPC1L	Yes
128	123	DDX6	Yes
139	153	4E-T	Yes
156	100	LSM14B	Yes
186	206	ZAR1	Yes

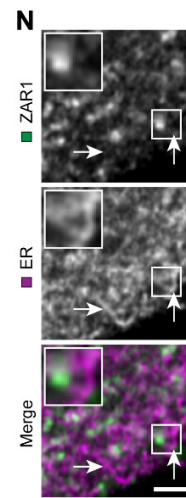
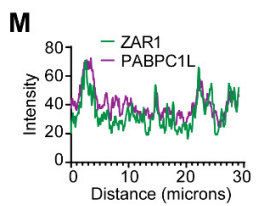
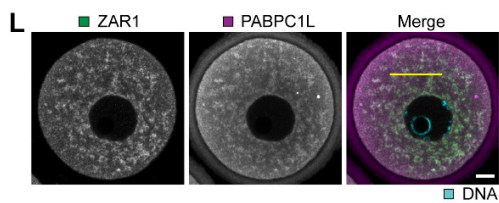
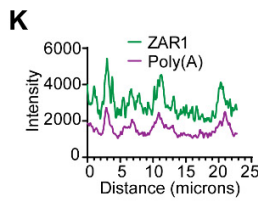
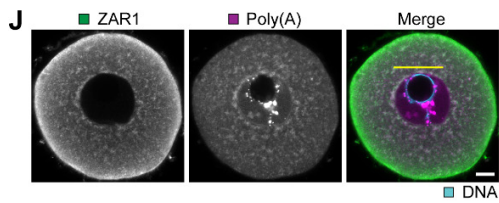
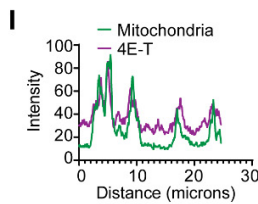
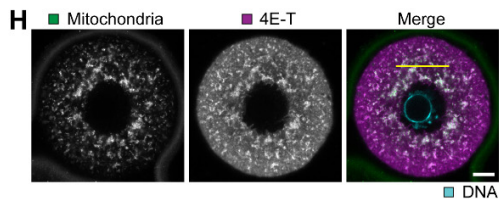
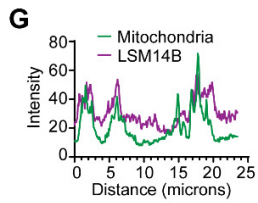
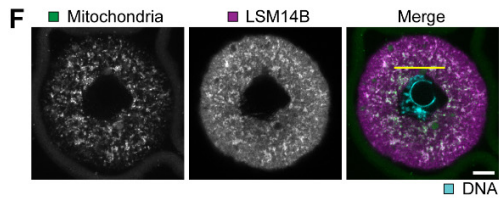
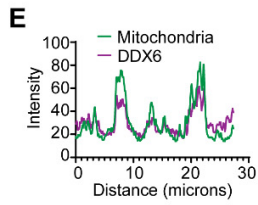
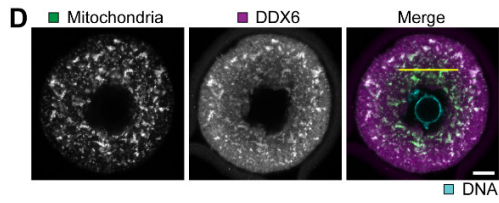
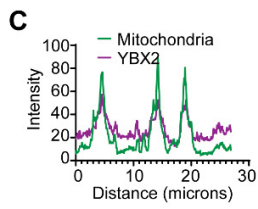
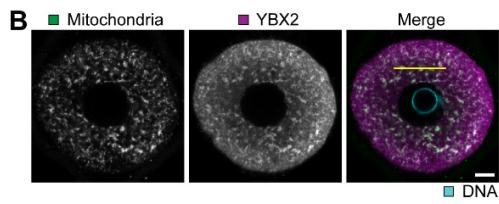


Figure S1

**Fig. S1.**

**Accumulation of RNA-binding proteins and mRNAs around mitochondria.** (A) Ranking of highly expressed RNA-binding proteins in all identified proteins in mouse oocytes. Proteins are ranked according to the LFQ (label-free quantitation) intensities. Two independent experiments with 1000 oocytes (1000oo) each were performed. (B-I) Representative immunofluorescence images of mouse GV oocytes (B, D, F, H). Green, mitochondria (cytochrome c (B, F, H), COX17 (D)); magenta, YBX2 (B), DDX6 (D), LSM14B (F), 4E-T (H); cyan, DNA (Hoechst 33342). Intensity profiles along the yellow lines are shown in (C, E, G, I) respectively. (J) Representative RNA FISH images of mouse GV oocytes. Oocytes were further stained with anti-ZAR1 antibody post FISH. Green, ZAR1; magenta, mRNAs with a poly(A) tail (5'-Cy5-Oligo d(T)30); cyan, DNA (Hoechst 33342). (K) Intensity profiles of ZAR1 and 5'-Cy5-Oligo d(T)30 along the yellow line in (J). (L) Representative immunofluorescence images of mouse GV oocytes. Green, ZAR1; magenta, PABPC1L (Poly(A) Binding Protein Cytoplasmic 1 Like); cyan, DNA (Hoechst 33342). (M) Intensity profiles of ZAR1 and PABPC1L along the yellow line in (L). (N) Representative immunofluorescence Airyscan images of mouse GV oocytes. Green, ZAR1; magenta, ER (BCAP31). Insets are magnifications of outlined regions. White arrows point to ER tubules that are not associated with ZAR1. Scale bars, 2  $\mu\text{m}$  for (N), 10  $\mu\text{m}$  for all the others.

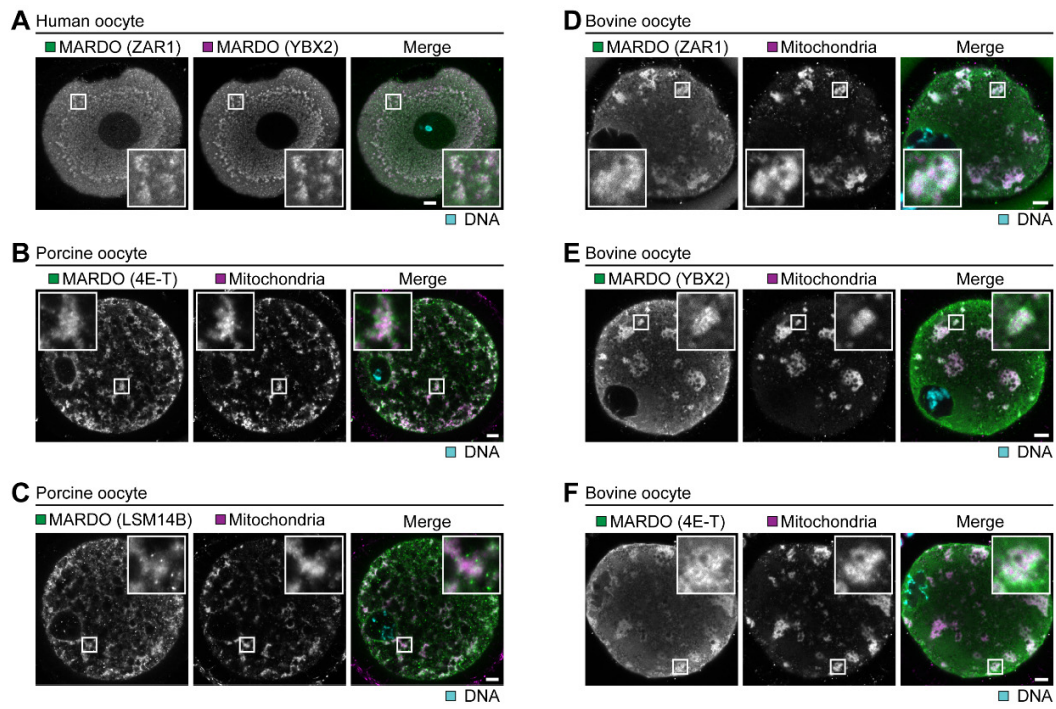


Figure S2

**Fig. S2.**

**The MARDO in human, porcine and bovine oocytes.** (A) Representative immunofluorescence images of human GV oocytes. Green, MARDO (ZAR1); magenta, MARDO (YBX2); cyan, DNA (Hoechst 33342). Insets are magnifications of outlined regions. (B and C) Representative immunofluorescence images of porcine GV oocytes. Green, MARDO (4E-T or LSM14B); magenta, mitochondria (TOMM20); cyan, DNA (Hoechst 33342). Insets are magnifications of outlined regions. (D-F) Representative immunofluorescence images of bovine GV oocytes. Green, MARDO (ZAR1, YBX2 or 4E-T); magenta, mitochondria (TOMM20); cyan, DNA (Hoechst 33342). Insets are magnifications of outlined regions. Scale bars, 10  $\mu\text{m}$ .

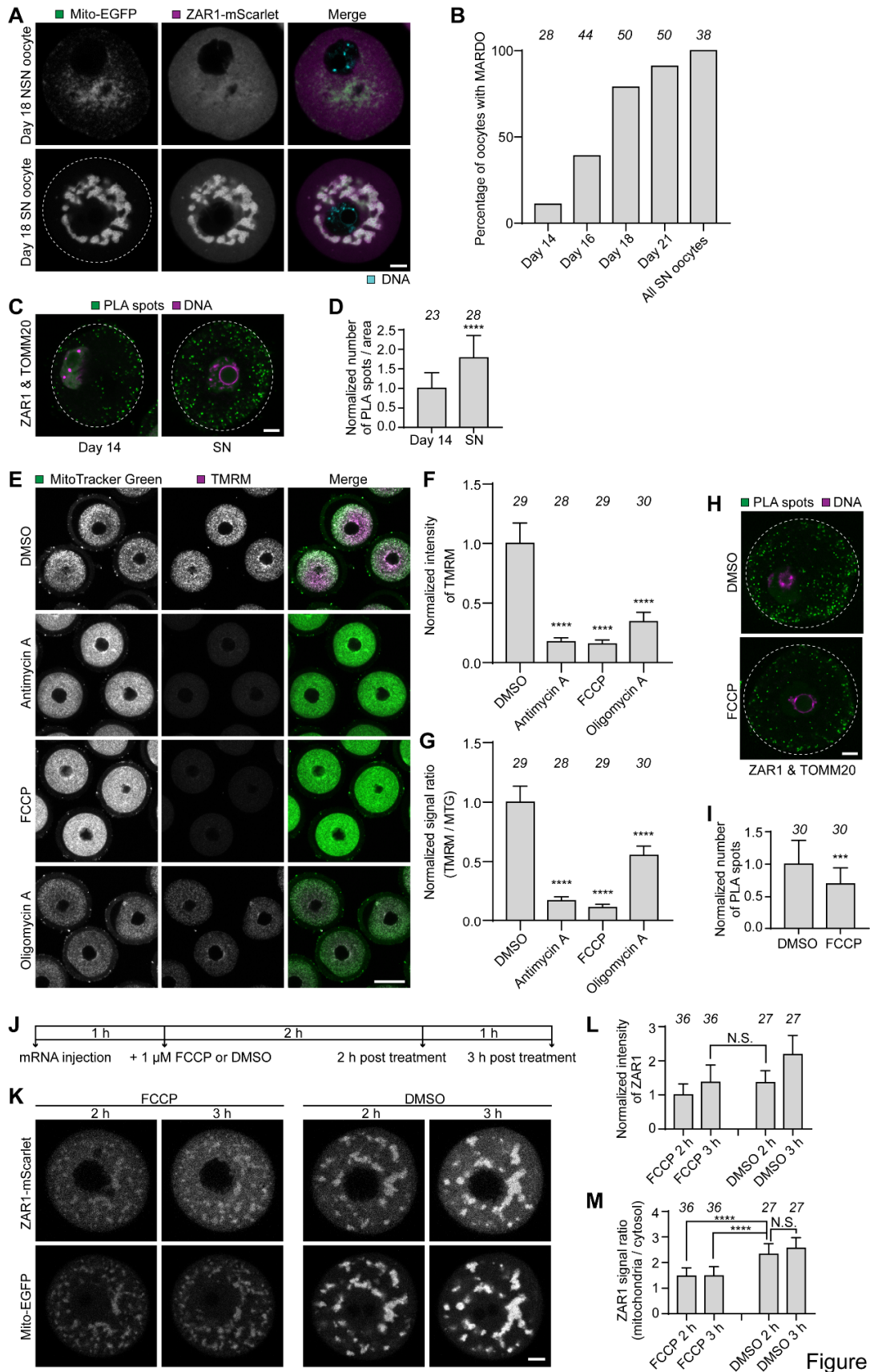


Figure S3

**Fig. S3.**

**MARDO formation during oocyte growth.** (A) Representative fluorescence images of NSN and SN mouse oocytes expressing Mito-EGFP (mitochondria, green) and ZAR1-mScarlet (MARDO, magenta), and stained with SiR-DNA (DNA, cyan). Oocytes were collected from 18-day-old mice. The dashed line demarcates the oocyte. (B) Quantification of the percentage of oocytes with MARDO labeled by ZAR-mScarlet. Oocytes were collected from mice of different ages. (C) Representative images of in situ PLA performed with the antibody pair anti-ZAR1 & anti-TOMM20 in early-stage oocytes collected from 14-day-old mice or SN oocytes collected from adult mice. Green, PLA spots; magenta, DNA (Hoechst 33342). Dashed lines demarcate the oocytes. (D) Quantification and normalization of the number of PLA spots. The number of PLA spots was divided by the area of the oocyte, because the size of early-stage oocyte differed from that of SN oocyte. The data were further normalized by dividing the values of each group by the mean of the first group (Day 14). (E) Representative fluorescence images of mouse GV oocytes stained with MitoTracker Geen (green) and TMRM (magenta). Oocytes were treated with DMSO, 5  $\mu$ g/ml Antimycin A, 5  $\mu$ M FCCP, or 5  $\mu$ g/ml Oligomycin A for 1 h at 37°C during staining. Scale bar, 50  $\mu$ m. (F) Quantification of the mean fluorescence intensity of TMRM. (G) Quantification of the fluorescence intensity ratio of TMRM to MitoTracker Green. (H) Representative images of in situ PLA performed with the antibody pair anti-ZAR1 & anti-TOMM20 in mouse GV oocytes. Oocytes were treated with DMSO or 5  $\mu$ M FCCP for 1 h at 37°C before fixation. Green, PLA spots; magenta, DNA (Hoechst 33342). Dashed lines demarcate the oocytes. (I) Quantification and normalization of the number of PLA spots. The data were normalized by dividing the values of each group by the mean of the first group (DMSO). (J) Schematic diagram of the experiment in (K). A lower concentration of FCCP was used here to allow the translation of ZAR1 during the first few hours. (K) Representative stills (mid-section) from time-lapse movies of mouse GV oocytes expressing ZAR1-mScarlet and Mito-EGFP. Oocytes were treated with 1  $\mu$ M FCCP or DMSO. Time is indicated as hours after drug treatment. (L) Quantification of the mean fluorescence intensity of ZAR1. (M) Quantification of the ratio of mean ZAR1 intensity on mitochondria to that in the cytosol. The ratio of signals on mitochondria relative to the cytosol is significantly lower in FCCP-treated oocytes when comparing oocytes with similar total ZAR1 protein levels (FCCP 3 h and DMSO 2 h; FCCP treatment leads to slower protein synthesis). The number of analyzed oocytes is specified in italics. Data are shown as mean  $\pm$  SD (D, F, G, I, L, M). *P* values were calculated using unpaired two-tailed Student's *t* test (D, I) or one-way ANOVA with Tukey's *post-hoc* test (F, G, L, M). Scale bars, 10  $\mu$ m unless otherwise specified.

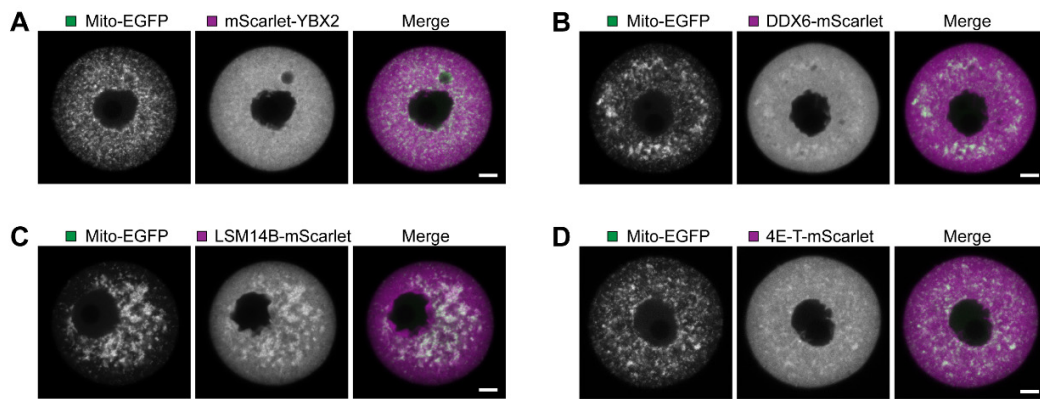


Figure S4

**Fig. S4.**

**Overexpression of YBX2, DDX6, LSM14B or 4E-T has no effect on mitochondrial clustering.**

(A-D) Representative fluorescence images of mouse GV oocytes. Green, Mito-EGFP (mitochondria); magenta, mScarlet-YBX2 (A), DDX6-mScarlet (B), LSM14B-mScarlet (C), 4E-T-mScarlet (D). Scale bars, 10  $\mu$ m.

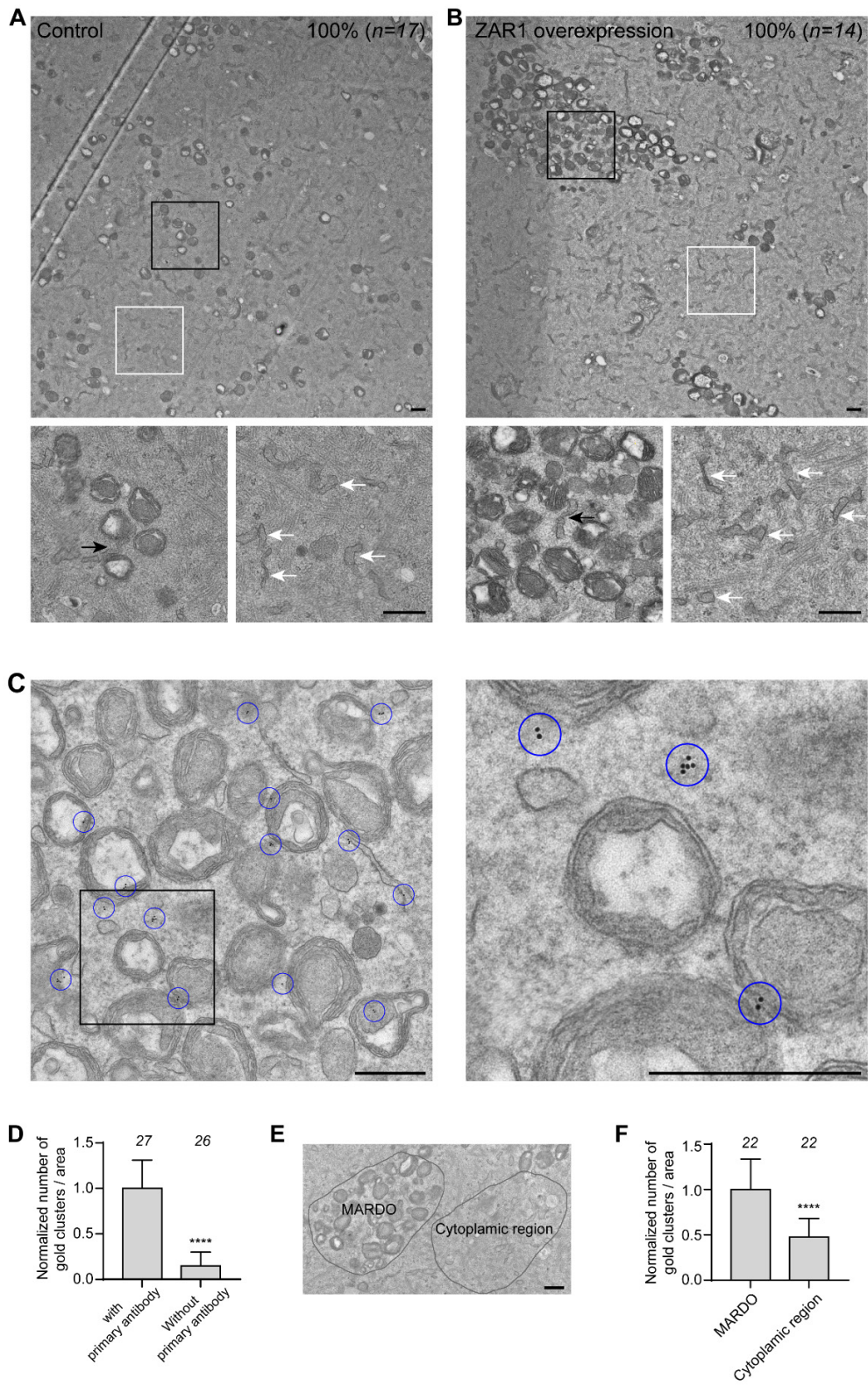


Figure S5

**Fig. S5.**

**ZAR1 overexpression promotes mitochondrial clustering.** (A) Representative transmission electron microscopy (TEM) images showing the distribution of mitochondria in mouse GV oocytes. Outlined regions are magnified at the bottom. The black arrow points to a mitochondria-associated ER tubule inside of a small mitochondrial cluster. White arrows point to ER tubules in the cytosol. (B) Representative TEM images showing the distribution of mitochondria in mouse GV oocytes overexpressing ZAR1. Outlined regions are magnified at the bottom. The black arrow points to a mitochondria-associated ER tubule inside of a large mitochondrial cluster. White arrows point to ER tubules outside of mitochondrial clusters. The percentage of TEM sections with representative patterns is shown in (A, B). “n” indicates the number of analyzed sections. (C) Representative immunoelectron microscopy images showing that ZAR1 is localized in the interstitial spaces within the mitochondrial cluster. The outlined region is magnified on the right. Gold clusters that label ZAR1 were marked with blue circles. (D) Comparison of the number of ZAR1 immuno-gold clusters in the MARDO in samples treated with or without primary antibody. The data were normalized by dividing the values of each group by the mean of the first group (with primary antibody). Very few gold clusters were observed in samples that were only stained with the gold-conjugated secondary antibody. (E) A representative immunoelectron microscopy image showing how the relative number of ZAR1 immuno-gold clusters in the MARDO and in the corresponding cytoplasmic region was quantified. (F) Comparison of the number of gold clusters in the regions of the MARDO and corresponding cytoplasmic regions outside the MARDO. The data were normalized by dividing the values of each group by the mean of the first group (MARDO). A significant enrichment of gold clusters in the regions of the MARDO was observed despite the fact that the mitochondria took up more than ~50% of the space in the MARDO regions. The number of analyzed mitochondrial clusters or cytoplasmic regions of the same size is specified in italics. Data are shown as mean  $\pm$  SD. *P* values were calculated using unpaired two-tailed Student’s *t* test. Scale bars, 0.5  $\mu$ m.

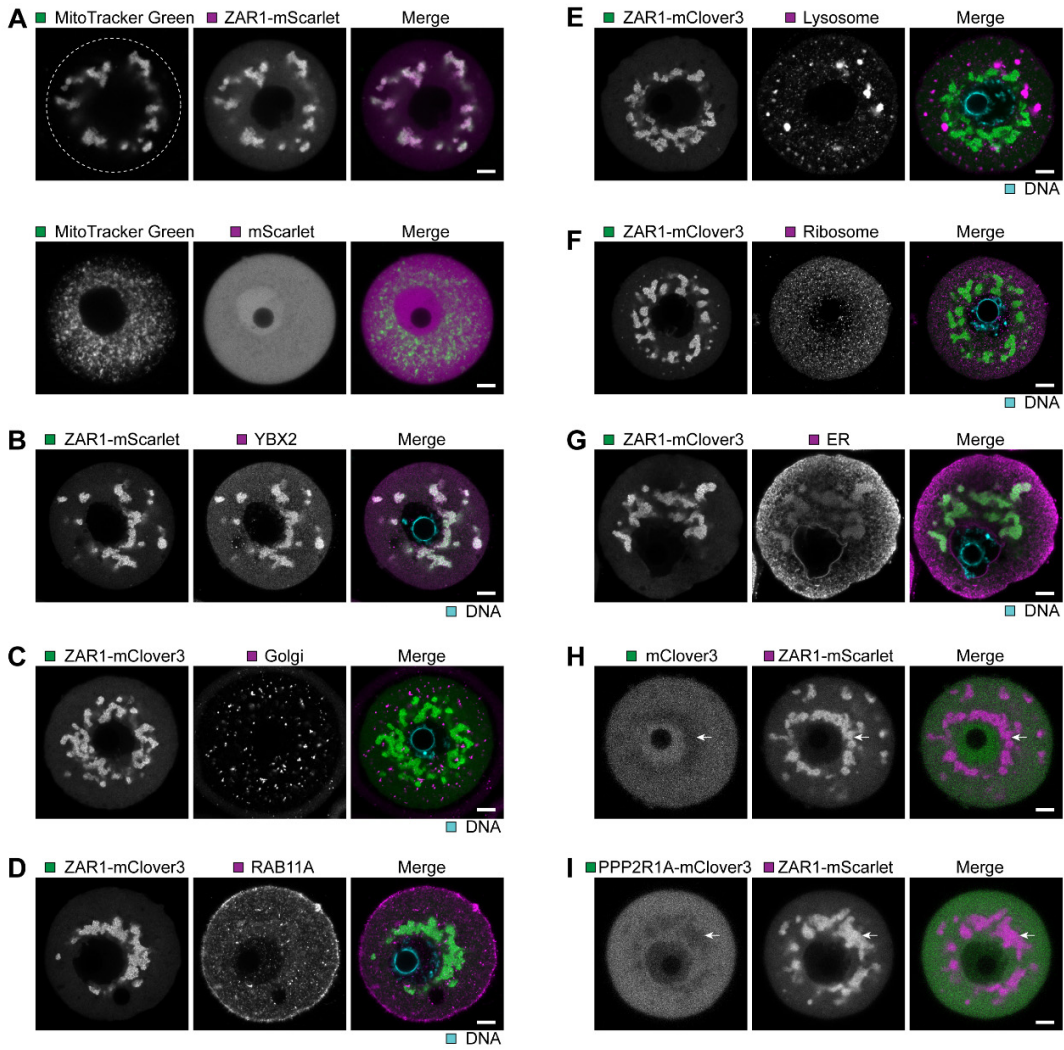


Figure S6

**Fig. S6.**

**The MARDO is exclusively associated with mitochondria.** (A) Representative fluorescence images of mouse GV oocytes overexpressing ZAR1-mScarlet or mScarlet (magenta). Oocytes were further stained with MitoTracker Green (mitochondria, green). The dashed line demarcates the oocyte. (B) Representative fluorescence images of mouse GV oocytes overexpressing ZAR1-mScarlet (MARDO, green). Oocytes were further stained with anti-YBX2 antibody (magenta). (C-G) Representative fluorescence images of mouse GV oocytes overexpressing ZAR1-mClover3 (MARDO, green). Oocytes were further stained with anti-GM130 (C), anti-RAB11A (D), anti-LAMP1 (E), anti-RPL24 (F), or anti-KDEL (G) antibody (magenta). (H) Representative fluorescence images of mouse GV oocytes overexpressing mClover3 (green) and ZAR1-mScarlet (MARDO, magenta). (I) Representative fluorescence images of mouse GV oocytes overexpressing PPP2R1A-mClover3 (green) and ZAR1-mScarlet (MARDO, magenta). Arrows point to the MARDO (H, I). Scale bars, 10  $\mu$ m.

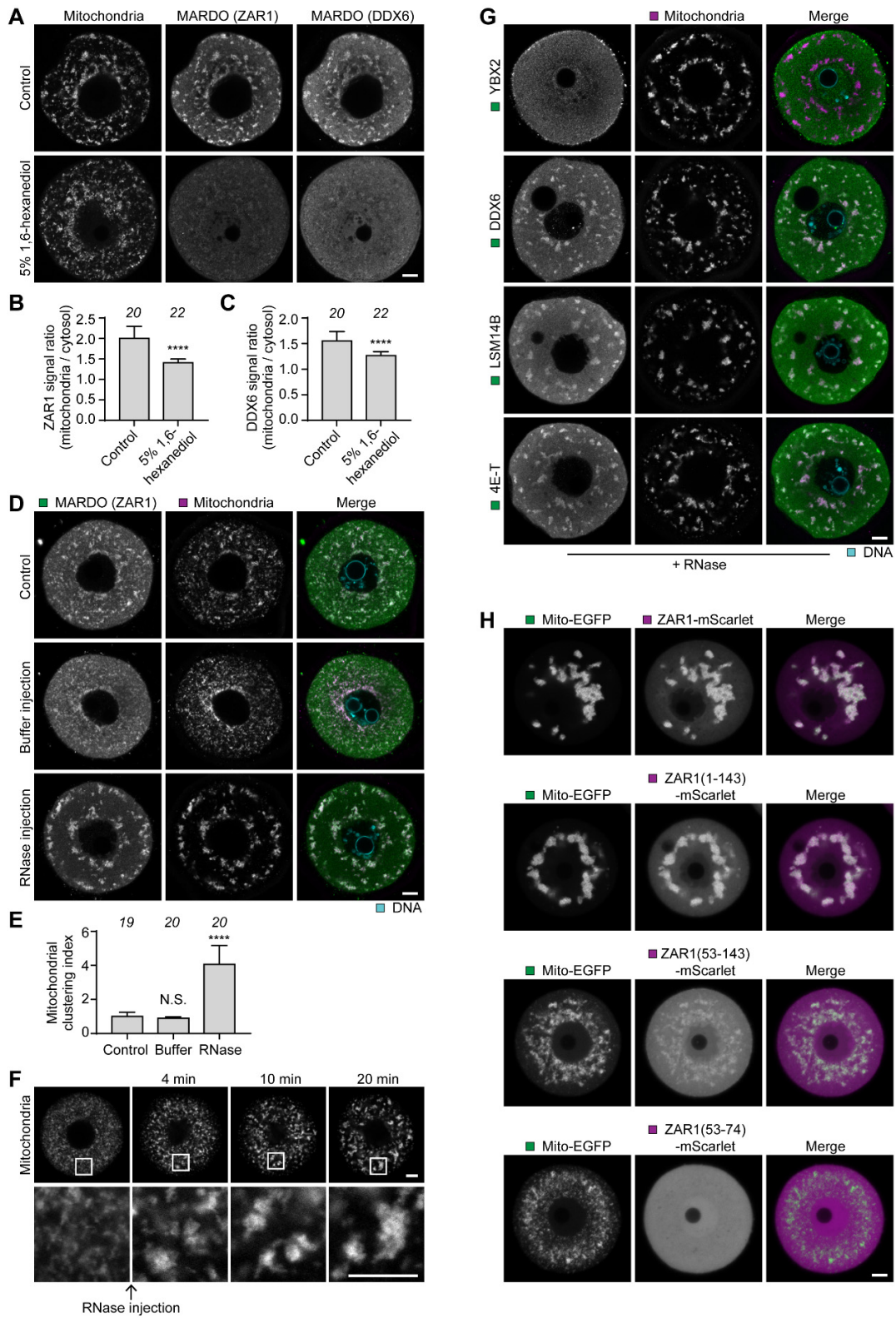


Figure S7

**Fig. S7.**

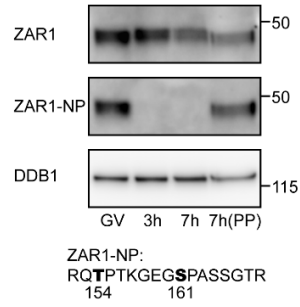
**RNase injection promotes MARDO coalescence and mitochondrial clustering.** (A) Representative immunofluorescence images of mouse GV oocytes. Oocytes were kept in culture medium (control) or treated with 5% 1,6-hexanediol in culture medium for 5 minutes at 37°C before fixation. Mitochondria were labeled with COX17. The MARDO was labeled with both ZAR1 and DDX6. Longer 1,6-hexanediol treatments harm oocytes. Therefore, oocytes were treated with 1,6-hexanediol for only 5 minutes and fixed immediately after treatment. Mitochondria did not have enough time to move substantially within this short time period. (B) Quantification of the ratio of mean ZAR1 intensity on mitochondria to that in the cytosol. (C) Quantification of the ratio of mean DDX6 intensity on mitochondria to that in the cytosol. (D) Representative immunofluorescence images of mouse GV oocytes injected with buffer or RNase. Oocytes were incubated at 37°C for half an hour after completion of injection. Non-injected oocytes were used as control. Green, MARDO (ZAR1); magenta, mitochondria (cytochrome c); cyan, DNA (Hoechst 33342). (E) Quantification of the mitochondrial clustering index. (F) Representative stills from time-lapse movies of mouse GV oocytes stained with TMRM. Oocytes were injected with RNase and imaged immediately after injection. Time is given as minutes after RNase injection. Outlined regions are magnified at the bottom. (G) Representative immunofluorescence images of mouse GV oocytes injected with RNase. Oocytes were fixed half an hour after injection. Green, YBX2, DDX6, LSM14B or 4E-T; magenta, mitochondria (cytochrome c); cyan, DNA (Hoechst 33342). (H) Representative fluorescence images of mouse GV oocytes expressing Mito-EGFP (mitochondria, green) and ZAR1-mScarlet, ZAR1(1-143)-mScarlet, ZAR1(53-143)-mScarlet, or ZAR1(53-74)-mScarlet (magenta). ZAR1 may undergo dimerization through the C-terminal domain (40), which may promote hydrogel formation mediated by the N-terminal domain. This might explain why full-length ZAR1 showed the most prominent localization on mitochondria and promoted mitochondrial clustering most strongly. The number of analyzed oocytes is specified in italics. Data are shown as mean  $\pm$  SD. *P* values were calculated using unpaired two-tailed Student's *t* test (B, C) or one-way ANOVA with Tukey's *post-hoc* test (E). Scale bars, 10  $\mu$ m.

**A** MI-stage-specific phosphorylation sites of MARDO proteins

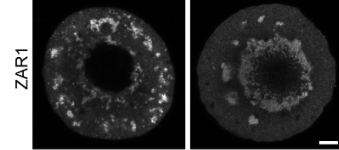
Protein name	Protein identifier	Position of phosphorylated amino acid		
		Identified from both 400oo and 1500oo	Identified only from 1500oo	Identified only from 400oo
DDX6	P54823	55		
EIF4ENIF1 (4E-T)	Q9EST3-1	86, 119, 344, 563, 890, 922	25, 135, 137, 212, 300, 373, 416, 454, 576, 586	
LSM14B	Q8CGC4	2, 154, 165	106, 115	
YBX2	Q9Z2C8-1	78, 218	67, 139, 203, 206,	351
ZAR1	Q80SU3		154, 161	

MI<sub>intensity</sub> / GV<sub>intensity</sub> > 4, PEP < 0.01, Phospho (STY) Probabilities > 0.9

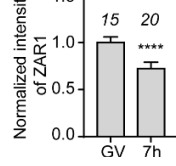
**B**



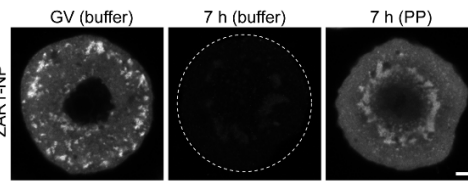
**C**



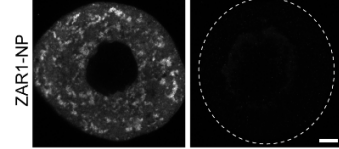
**D**



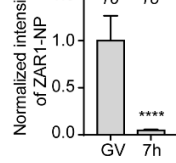
**G**



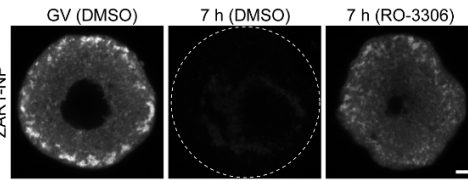
**E**



**F**



**H**



Treat oocytes just after NEBD

**I**

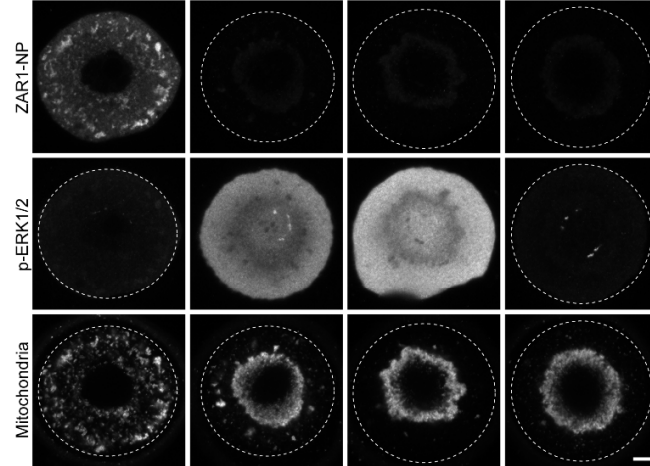


Figure S8

**Fig. S8.**

**Phosphorylation of MARDO proteins during the GV-MI transition.** (A) Phosphorylation of MARDO proteins during oocyte meiotic maturation. Two independent mass spectrometry analyses were performed. The first (400oo) used 400 GV oocytes and 400 MI oocytes, while the second (1500oo) used 1500 GV oocytes and 1500 MI oocytes. PEP: Posterior Error Probability of the identification. This value essentially operates as a p-value, where smaller is more significant. Phospho (STY) Probabilities: PTM positioning probabilities ([0..1], where 1 is best match) for “Phospho (STY)”. (B) Western blot analyses showing the expression of ZAR1 and the non-phosphorylated ZAR1 (ZAR1-NP) in mouse oocytes. Oocytes were lysed at different times after washout of dbcAMP. Lambda protein phosphatase (PP) treatment on cell lysate was performed before loading. DDB1 was used as a loading control. The antigen used to raise the “non-phosphorylated ZAR1”-specific antibody is shown below. (C) Representative immunofluorescence images of mouse oocytes stained with anti-ZAR1 antibody that recognizes all ZAR1 proteins. Oocytes were kept for 7 hours with dbcAMP (GV) or kept for 7 hours after washout of dbcAMP (7 h) before fixation. (D) Quantification of the mean fluorescence intensity of ZAR1. (E) Representative immunofluorescence images of mouse oocytes stained with anti-ZAR1-NP antibody. Oocytes were kept for 7 hours with dbcAMP (GV) or kept for 7 hours after washout of dbcAMP (7 h) before fixation. The dashed line demarcates the oocyte. (F) Quantification of the mean fluorescence intensity of non-phosphorylated ZAR1. (G) Representative immunofluorescence images of mouse oocytes stained with anti-ZAR1-NP antibody. Oocytes were kept for 7 hours with dbcAMP (GV) or kept for 7 hours after washout of dbcAMP (7 h) before fixation. Permeabilized oocytes were treated with Lambda protein phosphatase (PP) or PP buffer before staining. The dashed line demarcates the oocyte. (H) Representative immunofluorescence images of mouse oocytes stained with anti-ZAR1-NP antibody. Oocytes were kept for 7 hours with dbcAMP (GV) or kept for 7 hours after washout of dbcAMP (7 h) before fixation. GV oocytes were treated with DMSO. 7 h oocytes were treated with either DMSO or 10  $\mu$ M RO-3306 just after NEBD. The dashed line demarcates the oocyte. (I) Representative immunofluorescence images of mouse oocytes stained with anti-ZAR1-NP, anti-phospho-ERK1/2 and anti-cytochrome c (mitochondria) antibodies. Oocytes were kept for 7 hours with dbcAMP (GV) or kept for 7 hours after washout of dbcAMP (7 h) before fixation. GV oocytes were treated with DMSO. 7 h oocytes were treated with DMSO, 10  $\mu$ M MG-132 or 20  $\mu$ M U-0126 after washout of dbcAMP. Dashed lines demarcate the oocyte. The number of analyzed oocytes is specified in italics. Data are shown as mean  $\pm$  SD. *P* values were calculated using unpaired two-tailed Student’s *t* test. Scale bars, 10  $\mu$ m.

**A** Phosphorylation sites of ZAR1 by CDK1-Cyclin B1 (*in vitro*)

Phospho (STY) Probabilities	Residues	PEP	Score
TLQPAGCRAS(1)PDAR	S105	2.59E-43	205.45
GHAGAGRS(1)PR	S124	3.46E-14	164.90
QT(1)PTKGEKSPASSGTR	T154	1.13E-56	213.51
GEGS(1)PASSGTREPEPR	S161	1.91E-140	306.96
DQAS(1)PQSTEQDKER	S244	5.29E-116	285.98

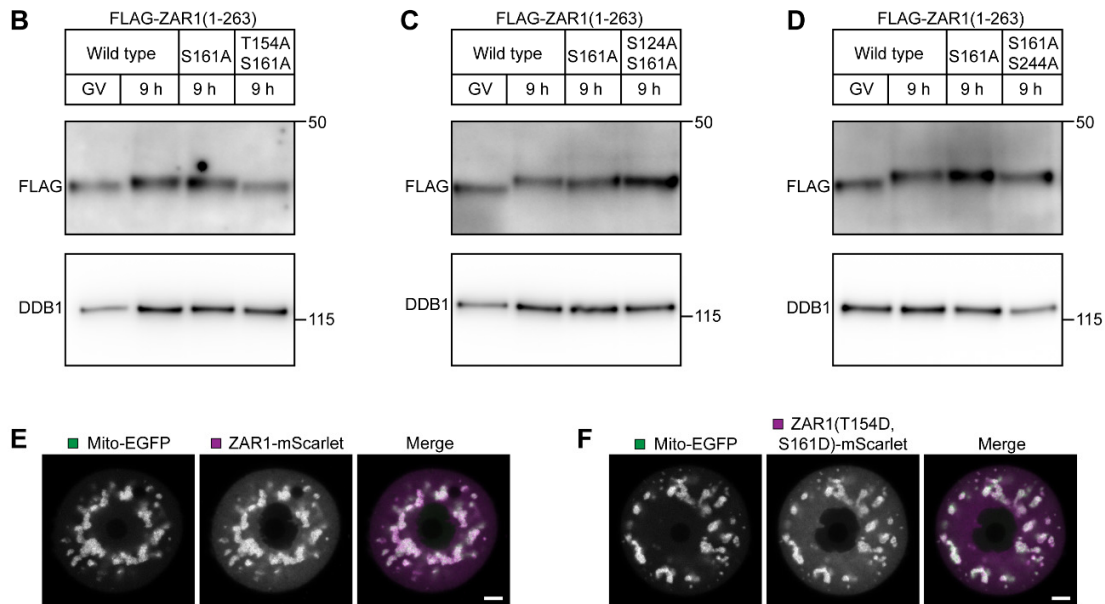


Figure S9

**Fig. S9.**

**Identification of ZAR1 phosphorylation sites by CDK1.** (A) In vitro phosphorylation assay reveals phosphorylation sites of ZAR1 by CDK1-cyclin B1. Only phosphorylation sites that match the minimal consensus motif Ser/Thr-Pro (S/T-P) phosphorylatable by CDK1 are shown. Phospho (STY) Probabilities: sequence representation of the peptide including PTM positioning probabilities ([0..1], where 1 is best match) for “Phospho (STY)”. Residues: the amino acid position of the phosphorylated residue within the protein. PEP: Posterior Error Probability of the identification. This value essentially operates as a p-value, where smaller is more significant. Score: Andromeda score for the best associated MS/MS spectrum. (B-D) Western blot analyses showing the expression of overexpressed FLAG-ZAR1(1-263) variants in mouse oocytes. Oocytes were lysed at different times after washout of dbcAMP. DDB1 was used as a loading control. (E and F) Representative fluorescence images of mouse GV oocytes expressing mito-EGFP (green) and ZAR1-mScarlet or ZAR1(T154D, S161D)-mScarlet (magenta). Scale bars, 10  $\mu$ m.

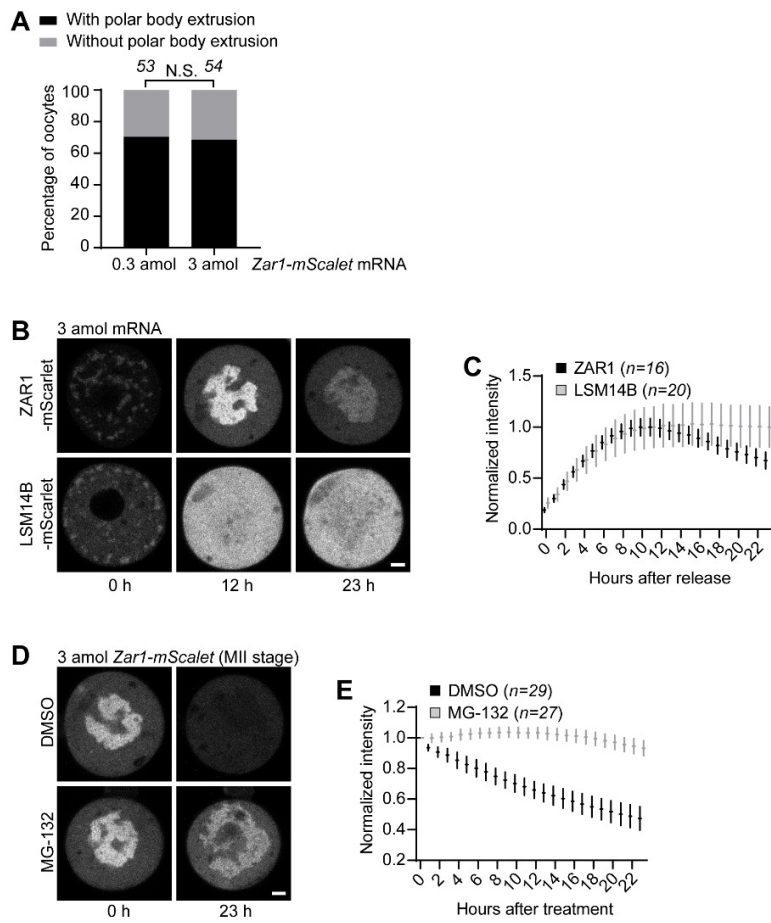


Figure S10

**Fig. S10.**

**Proteasomal degradation of ZAR1 is essential for MARDO dissolution.** (A) Quantification of polar body extrusion of mouse oocytes with 0.3 amol or 3 amol *Zar1-mScarlet* mRNA injected at GV stage. (B) Representative stills (mid-section) from time-lapse movies of mouse oocytes with 3 amol *Zar1-mScarlet* or *Lsm14b-mScarlet* mRNA injected. Time is given as hours after washout of dbcAMP. (C) Quantification of the total fluorescence intensity (21 sections every 3  $\mu\text{m}$ ) of ZAR1 and LSM14B. (D) Representative stills (mid-section) from time-lapse movies of mouse MII oocytes expressing ZAR1-mScarlet. 3 amol *Zar1-mScarlet* mRNA was injected into GV oocytes. 3 hours later, oocytes were transferred to dbcAMP-free medium for in vitro maturation. 15 hours later, in vitro matured MII oocytes were either treated with DMSO or 10  $\mu\text{M}$  MG-132 for live cell imaging. Time is given as hours after drug treatment. (E) Quantification of the total fluorescence intensity (25 sections every 3  $\mu\text{m}$ ) of ZAR1. The number of analyzed oocytes is specified in italics. Data are shown as mean  $\pm$  SD (C, E). *P* values were calculated using Fisher's exact test (A). Scale bars, 10  $\mu\text{m}$ .

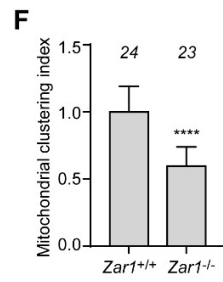
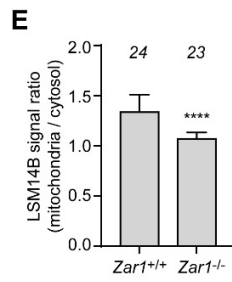
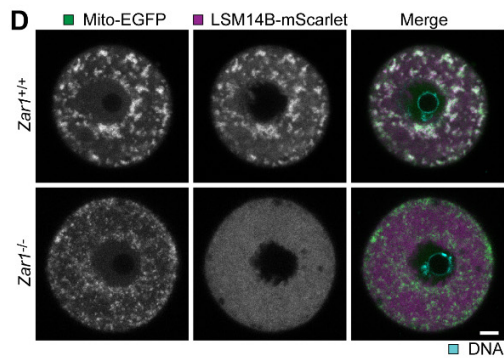
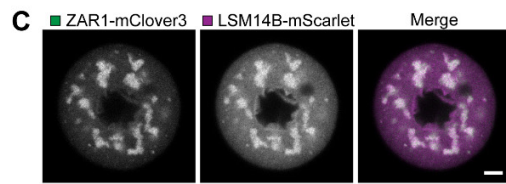
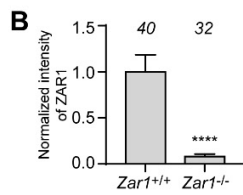
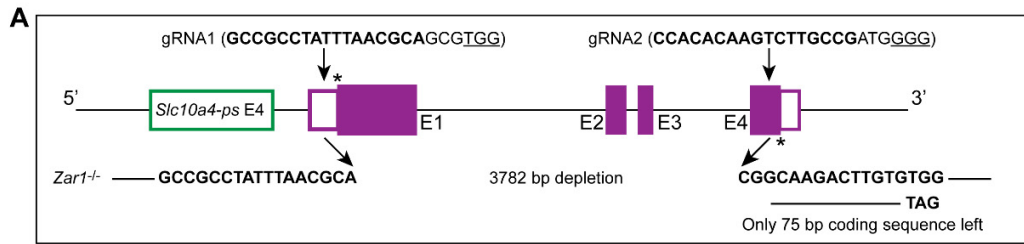


Figure S11

**Fig. S11.**

***Zar1* knockout impairs MARDO formation and mitochondrial clustering.** (A) Schematic representation showing the gene targeting strategy for *Zar1* knockout mice. Solid magenta bars represent four exons (E1, E2, E3, and E4) of *Zar1*. Hollow magenta bars represent 5' and 3' UTR. The DNA sequence of *Zar1* knockout mouse and the corresponding gRNA sequences are shown in bold. gRNA, guide RNA; \*, start or stop codon. (B) Quantification of the mean fluorescence intensity of ZAR1 (C) Representative fluorescence images of mouse GV oocytes expressing ZAR1-mClover3 (green) and LSM14B-mScarlet (magenta). (D) Representative fluorescence images of GV oocytes expressing Mito-EGFP (mitochondria, green) and LSM14B-mScarlet (MARDO, magenta) collected from *Zar1*<sup>+/+</sup> and *Zar1*<sup>-/-</sup> mice. (E) Quantification of the ratio of mean LSM14B intensity on mitochondria to that in the cytosol. (F) Quantification of the mitochondrial clustering index. The number of analyzed oocytes is specified in italics. Data are shown as mean ± SD. *P* values were calculated using unpaired two-tailed Student's *t* test. Scale bars, 10 μm.

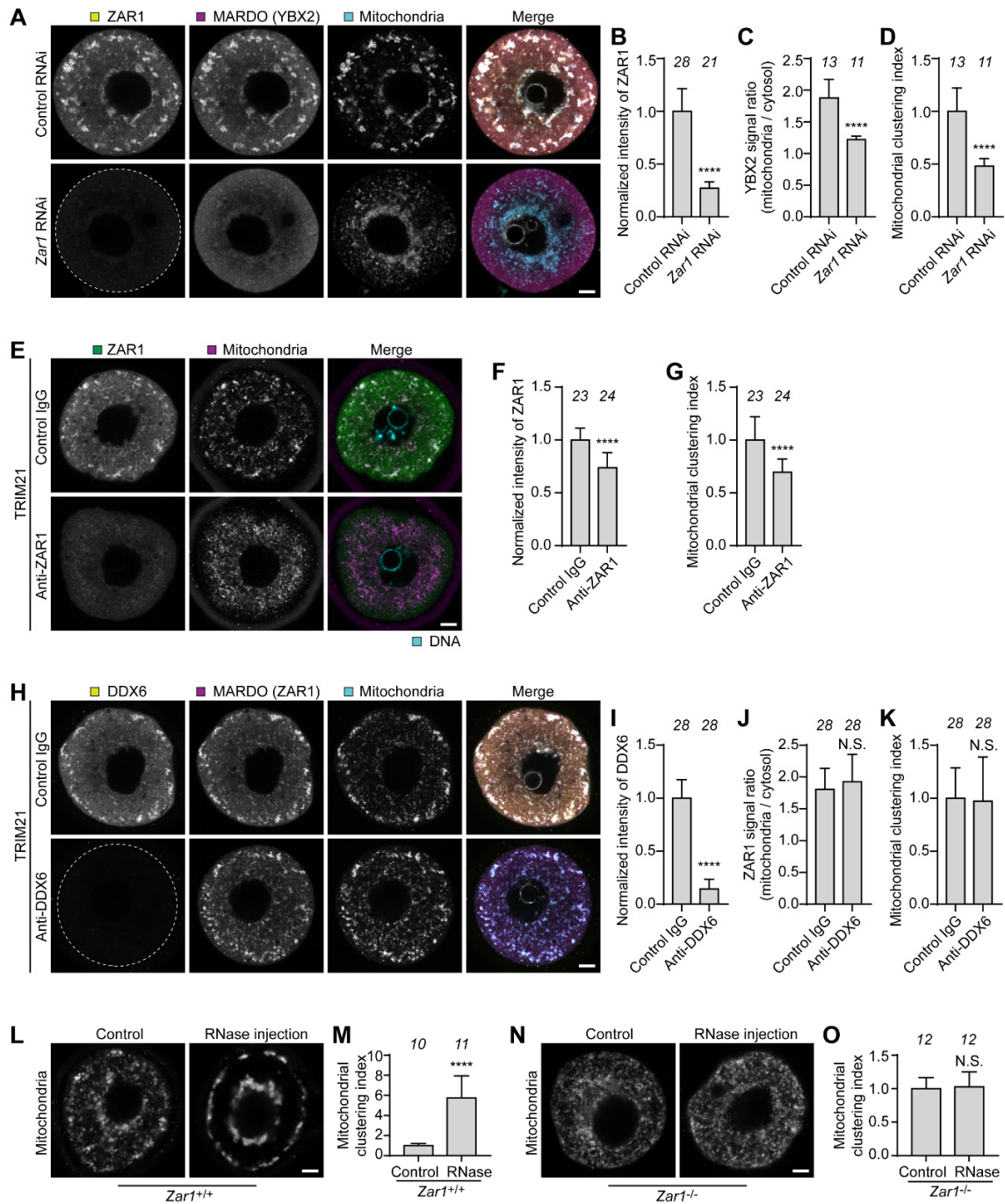


Figure S12

**Fig. S12.**

**Zar1** down-regulation impairs MARDO formation and mitochondrial clustering. **(A)** Representative immunofluorescence images of control RNAi and *Zar1* RNAi mouse GV oocytes. Yellow, ZAR1; magenta, MARDO (YBX2); cyan, mitochondria (cytochrome c). The dashed line demarcates the oocyte. **(B)** Quantification of the mean fluorescence intensity of ZAR1 **(C)** Quantification of the ratio of mean YBX2 intensity on mitochondria to that in the cytosol. **(D)** Quantification of the mitochondrial clustering index. **(E)** Representative immunofluorescence images of control and ZAR1-depleted mouse GV oocytes by Trim-Away. Green, ZAR1; magenta, mitochondria (cytochrome c); cyan, DNA (Hoechst 33342). **(F)** Quantification of the mean fluorescence intensity of ZAR1. **(G)** Quantification of the mitochondrial clustering index. **(H)** Representative immunofluorescence images of control and mouse GV oocytes depleted of DDX6 by Trim-Away. Yellow, DDX6; magenta, MARDO (ZAR1); cyan, mitochondria (COX17). The dashed line demarcates the oocyte. **(I)** Quantification of the mean fluorescence intensity of DDX6. **(J)** Quantification of the ratio of mean ZAR1 intensity on mitochondria to that in the cytosol. **(K)** Quantification of the mitochondrial clustering index. **(L)** Representative immunofluorescence images of *Zar1*<sup>+/+</sup> GV oocytes with or without RNase injection. Oocytes were fixed half an hour after injection and were then stained with anti-cytochrome c (mitochondria) antibody. **(M)** Quantification of the mitochondrial clustering index. **(N)** Representative immunofluorescence images of *Zar1*<sup>-/-</sup> GV oocytes with or without RNase injection. Oocytes were fixed half an hour after injection and were then stained with anti-cytochrome c (mitochondria) antibody. **(O)** Quantification of the mitochondrial clustering index. The number of analyzed oocytes is specified in italics. Data are shown as mean ± SD. *P* values were calculated using unpaired two-tailed Student's *t* test. Scale bars, 10 μm.

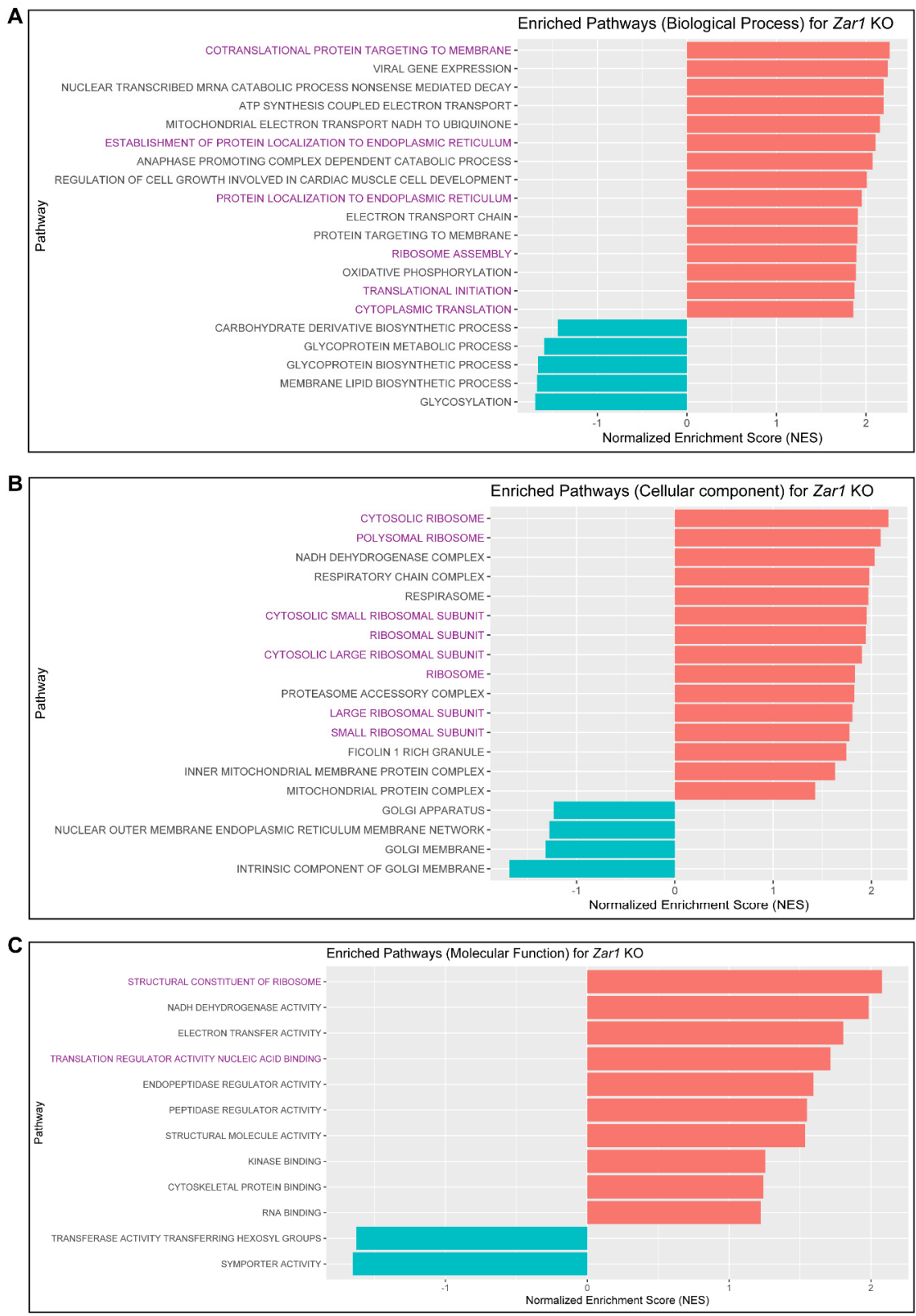


Figure S13

**Fig. S13.**

**Gene ontology analysis on RNA-seq data of *Zar1*<sup>+/+</sup> and *Zar1*<sup>-/-</sup> oocytes.** (A-C) Up-regulated (orange bars) and down-regulated (cyan bars) pathways (biological process (A), cellular component (B), molecular function (C)) in *Zar1*<sup>-/-</sup> oocytes versus *Zar1*<sup>+/+</sup> oocytes. Magenta terms are translation-related pathways.

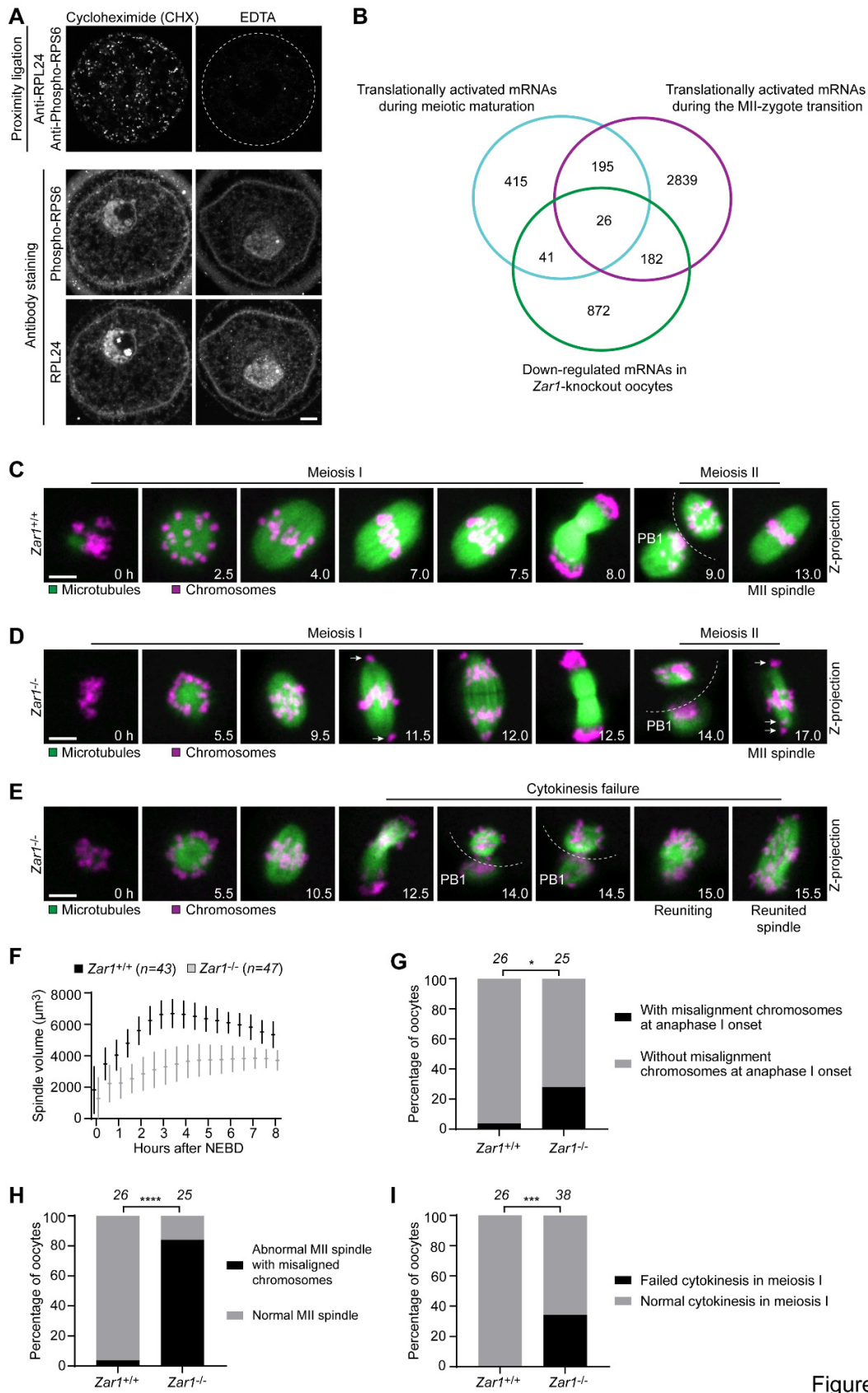
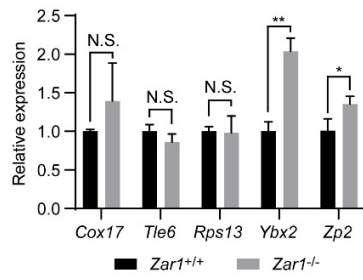


Figure S14

**Fig. S14.**

**MARDO disruption causes premature loss of mRNAs for future use and defects of meiosis.**

(A) Representative images of in situ PLA performed with antibody pair anti-RPL24 & anti-Phospho-RPS6 in mouse GV oocytes (top panel). Representative immunofluorescence images of mouse GV oocytes stained with anti-RPL24 and anti-Phospho-RPS6 antibodies (bottom panel). Oocytes were permeabilized and treated with cycloheximide (CHX) that stabilizes ribosomes or EDTA that causes ribosome disassembly before fixation. (B) Venn diagrams showing the overlap in transcripts. Cyan, translationally activated mRNAs during oocyte meiotic maturation, log<sub>2</sub> fold-change > 1 (8 h versus 0 h post-meiotic resumption); magenta, translationally activated mRNAs during the MII-zygote transition, log<sub>2</sub> fold-change > 1 (zygotes versus MII oocytes); green, down-regulated mRNAs in *Zar1*-knockout oocytes, log<sub>2</sub> fold-change < -1 (*Zar1*<sup>-/-</sup> versus *Zar1*<sup>+/+</sup> oocytes). (C-E) Representative stills from time-lapse movies of *Zar1*<sup>+/+</sup> and *Zar1*<sup>-/-</sup> oocytes. Green, microtubules (mClover3-MAP4-MTBD); magenta, chromosomes (H2B-mRFP). Time is indicated as hours after NEBD. PB1, the first polar body. Arrows highlight misaligned chromosomes. Dashed lines separate the oocyte and polar body. Z projections, 37 sections every 2 μm. (F) Quantification of spindle volume in *Zar1*<sup>+/+</sup> and *Zar1*<sup>-/-</sup> mouse oocyte. (G) Quantification of chromosome misalignment at anaphase I onset in *Zar1*<sup>+/+</sup> and *Zar1*<sup>-/-</sup> mouse oocyte. (H) Quantification of abnormal MII spindle with misaligned chromosomes in *Zar1*<sup>+/+</sup> and *Zar1*<sup>-/-</sup> mouse oocyte. (I) Quantification of cytokinesis failure in *Zar1*<sup>+/+</sup> and *Zar1*<sup>-/-</sup> mouse oocyte. The number of analyzed oocytes is specified in italics. Data are shown as mean ± SD (F). *P* values were calculated using Fisher's exact test (G, H, I). Scale bars, 10 μm.



**Fig. S15.**

**Examples of mRNAs that are not down-regulated in *Zar1*-knockout oocytes.** RT-qPCR results showing expression of five genes (*Cox17*, *Tle6*, *Rps13*, *Ybx2*, and *Zp2*) in *Zar1*<sup>+/+</sup> and *Zar1*<sup>-/-</sup> oocytes. Three biological replicates were used in the experiment. Data are shown as mean ± SD. *P* values were calculated using unpaired two-tailed Student's *t* test.